arXiv:2505.00538v1 [cond-mat.mes-hall] 1 May 2025

Dynamical control of random telegraph noise in magnetic tunnel junctions

Mehrdad Elyasi,[1,2,*] Shun Kanai,[3,1,2,4,5,6] Hideo Ohno,[2,7] Shunsuke Fukami,[3,1,2,7,8] and Gerrit E. W. Bauer[1,2,9]

[1] *Advanced Institute for Materials Research, Tohoku University, Sendai 980-8577, Japan*
[2] *Center for Science and Innovation in Spintronics, Tohoku University, 2-1-1 Katahira, Sendai 980-8577, Japan.*
[3] *Laboratory for Nanoelectronics and Spintronics, Research Institute of Electrical Communication, Tohoku University, 2-1-1 Katahira, Sendai 980-8577, Japan*
[4] *PRESTO, Japan Science and Technology Agency (JST), Kawaguchi 332-0012, Japan.*
[5] *Division for the Establishment of Frontier Sciences of Organization for Advanced Studies at Tohoku University, Tohoku University, Sendai 980-8577, Japan.*
[6] *National Institutes for Quantum Science and Technology.*
[7] *Center for Innovative Integrated Electronic Systems, Tohoku University, 468-1 Aramaki Aza Aoba, Sendai 980-8572, Japan.*
[8] *Inamori Research Institute of Science, Shijo, Shimogyo-ku, Kyoto 600-8411, Japan.*
[9] *Kavli Institute for Theoretical Sciences, University of the Chinese Academy of Sciences, Beijing 10090, China*

Rapid random telegraph noise (RTN) in magnetic tunnel junctions (MTJs) is an important figure of merit for probabilistic computing applications. However, the interactions between the macrospin and spin waves with finite wave numbers reduce the RTN attempt frequency. We theoretically show that mode-selective heating and cooling can substantially tune the RTN frequency. We propose a nonlinear cooling mechanism that accelerates the switching dynamics. We outline experimental pathways to characterize the physics of nonlinear effects on RTN and to maximize the operation speed of MTJ-based probabilistic computing.

I. INTRODUCTION

The random telegraph noise (RTN) of magnetization arising from stochastic switching [1–9] has found application in probabilistic computing [10–16]. In the field of magnetism, the most common realization of probabilistic bits is based on the RTN associated with the switching of the entire magnetization of the free layer in magnetic tunnel junctions (MTJs), which are readily scalable down to few nanometer cross sections [17–19]. The stochastic switching of parametrically driven spin waves (magnon quasiparticles) in the phase space, offers an alternative realization of RTN in magnetic systems [20–22]. Magnonic fluctuations are also fundamental to the expanding field of quantum magnonics [23–27]. The large magnetization fluctuations associated with the magnetization reversal and the small fluctuations of magnons are not independent.

Brown [2, 3] addressed the distribution function of the macrospin directions around minima of the free energy and computed the switching frequencies using Kramers' escape approximations [28]. Inspired by experiments [29, 30], we argued that the nonlinear interaction of the macrospin with spin waves slows the magnetization RTN [31] by increasing the attempt time τ_0 in the Arrhenius law $\tau_s = \tau_0 e^{E_B/(k_B T_{env})}$ [32], where $f_s = 1/\tau_s$ is the switching frequency, E_B is the energy barrier, k_B is the Boltzmann constant, and T_{env} is the environment temperature. Since magnitude of the effect depends on the amplitude of the nonuniform magnon fluctuations, selectively reducing their (effective) temperature should decrease τ_0.

Here we outline mechanisms to control the RTN by actively manipulating magnon fluctuations by microwaves, rather than using passive methods such as tuning the magnetic field or anisotropy [4, 33–35]. Parametric excitation [see Sec. II] increases the magnon fluctuations, while we suggest reducing them by four-magnon interactions [see Sec. III]. Parametric excitation of the Kittel mode or macrospin [Sec. II A] enhances f_s, while exciting spin waves decreases it [Sec. II B]. The in-situ mode-selective cooling mechanism introduced in Sec. III A, increases f_s as seen in Sec. III B. In Sec. IV, we suggest concrete experiments that can test our predictions.

II. PARAMETRIC EXCITATION AND MAGNETIZATION RTN

Below the threshold power, parametric excitation of spin waves squeezes (squashes) the fluctuations, whereas above it, sustained oscillations emerge that are in-phase or out-of-phase with the microwave drive [20, 22, 36–38]. This bistability exhibits random telegraph noise by the stochastic switching between the two phases [21, 22], analogous to the MTJs in which the magnetization RTN occurs between two degenerate ground states on the Bloch sphere. Here, we establish a connection between the fluctuations of these two types of probabilistic bits (p-bits).

* mehrdad.elyasi.b2@tohoku.ac.jp

A. Macrospin excitation

In order to pin down the effect of nonlinear magnon interactions (see Sec. II B), we set the stage by considering the pure macrospin model RTN (without spin waves) with attempt time [3]

$$\tau_0 = F(\alpha_G, M_s, \lambda_{sd,\theta}, \lambda_{sd,\phi})[\sqrt{\lambda_{i,\phi}\lambda_{i,\theta}}]^{-1}, \quad (1)$$

where $\lambda_{x,y} = (\partial^2 E/\partial y^2)|_{\theta_x}$, $x \in \{sd, 1, 2\}$, $y \in \{\theta, \phi\}$, (θ, ϕ) are the azimuthal and polar angles from the easy axis. 'sd' refers to the saddle point of the free energy $E(\theta, \phi)$ of the macrospin, while '1' and '2' denote two equivalent energy minima. We group the dependence on the Gilbert damping constant α_G, saturation magnetization M_s, and curvature at the saddle points $\lambda_{sd,\theta(\phi)}$ into the function F.

MTJs can be parametrically excited directly by photons or by fast actuation of the anisotropy [see Sec. IV]. The Wigner distribution function of the Kittel mode in the absence of any drive and nonlinear interactions,

$$W_0 = \mathcal{N}' \exp[-2(X_0^2 + Y_0^2)/n_{th,0}], \quad (2)$$

where $\mathcal{N}'$ is a normalization constant, $X_{\vec{k}} = (c_{\vec{k}} + c_{\vec{k}}^\dagger)/2$, $Y_{\vec{k}} = -i(c_{\vec{k}} - c_{\vec{k}}^\dagger)/2$, $c_{\vec{k}}$ is the annihilation operator of the magnon with wave vector $\vec{k}$, and $n_{th,\vec{k}}$ is the thermal occupation of its environment. A magnetic field polarized parallel to the easy axis excites the macrospin when tuned to the frequency $2\omega_0$, where ω_0 is the ferromagnetic resonance frequency. Such excitation is governed by the $\mathcal{H}_{p,0} = P_0 c_0 c_0 + \text{H.c.}$. In the rotating frame of the Kittel mode frequency, the distribution function in the presence of the drive and dissipation becomes,

$$W_{0,P} = \mathcal{N} \exp\left\{ \frac{-2}{n_{th,0}} \left[-(1 + \text{Im}[\epsilon_0])X_0^2 - (1 - \text{Im}[\epsilon_0])Y_0^2 + 2\text{Re}[\epsilon_0]X_0 Y_0 \right] \right\}, \quad (3)$$

where $\mathcal{N}$ is a normalization constant. $\epsilon_0 = P_0/\xi_0$, where $\xi_{\vec{k}}$ is the dissipation rate of the magnon mode with wave vector $\vec{k}$.

Without loss of generality, we assume P_0 and thereby ϵ_0, to be imaginary. The second derivatives of the distribution function at the energy minima, i.e., prefactors of X_0^2 and Y_0^2 in the exponent, modify $\tau_0 \propto (\lambda_{1(2),\theta}\lambda_{1(2),\phi})^{-1/2} \propto (1 - |\epsilon_0|^2)^{-1/2}$. A larger parametric excitation $|P_0|$, therefore increases τ_0. On the other hand, since $\langle n_0 \rangle$ increases with $|P_0|$ beyond the thermal occupation, the energy minima effectively increase and lower E_B. Far below threshold, $\langle n_0 \rangle = n_{th,0}(1 - |\epsilon_0|^2)^{-1}$, so

$$\tau_s = \tau_{0,0}\sqrt{\frac{1}{1 - |\epsilon_0|^2}} \exp\left[\frac{E_{B,0}}{k_B T} - \frac{|\epsilon_0|^2}{1 - |\epsilon_0|^2} \right], \quad (4)$$

where $\tau_{0,0}$ and $E_{B,0}$ are the attempt time and energy barrier in equilibrium, respectively. When $(1 - |\epsilon_0|^2)^{-1/2} < \exp[|\epsilon_0|^2/(1 - |\epsilon_0|^2)]$, τ_s decreases with increasing drive. Close to the threshold and beyond, the above arguments should still hold, since quantities such as $\langle n_0 \rangle$ are regulated by the nonlinearities and abrupt changes should not occur [see Sec. II B].

To assess the high energy barrier approximation implicit in Kramers' escape model for the macrospin, we numerically solve the stochastic LLG equation for the macrospin as a function of P_0/ξ_0 under parametric microwave excitation for an in-plane (IP) equilibrium magnetization governed by an IP shape easy-axis and an out-of-plane (OOP) hard-axis anisotropy. An alternative would be an OOP equilibrium magnetization with easy-axis OOP and an in-plane shape anisotropy. Both cases were reported for the free layers in MTJs [4, 29, 30]. Here and below we focus on the former with $H_{K_h} = \mu_0 M_s K_h = 0.2\,\text{T}$ and $H_{K_e} = \mu_0 M_s K_e = -7.5\,\text{mT}$ [4, 29], respectively, where $M_s = 1.5 \times 10^6\,\text{A/m}$ is the saturation magnetization and K_e (K_h) is the easy (hard) axis anisotropy constant. We adopt a Gilbert damping constant $\alpha_G = 0.05$, and the sample radius (thickness) 10 nm (2 nm), unless stated otherwise. Here, we assume that the equilibrium magnetization $\vec{m}_{eqb}$ is along the easy axis. Figure 1(a) illustrates the increase of $f_{s,norm}$ and $\langle n_{0,norm} \rangle$ with $|P_0|$, where 'norm' refers to normalization with respect to the equilibrium values. According to Figure 1(b), $\tau_{0,norm}$ increases while $E_{B,norm}$ decreases with $|P_0|$ as expected.

B. $\pm\vec{k} \neq 0$ excitation

We argued previously [31] that the suppression of the RTN frequency is governed by the parameter

$$\xi_{corr} = \frac{2\xi_{\pm\mathcal{K}}\mathcal{D}_{suhl}^2(2\langle n_0 \rangle + 1)(2\langle n_{\pm\mathcal{K}} \rangle + 1)}{\Delta\omega_{\pm\mathcal{K}}^2 + \xi_{\pm\mathcal{K}}^2}, \quad (5)$$

where $\xi_{\vec{k}} = \alpha_G \omega_{\vec{k}}$ is the dissipation rate of a magnon with frequency $\omega_{\vec{k}}$, $n_{\vec{k}} = c_{\vec{k}}^\dagger c_{\vec{k}}$ is the number operator, $\langle O \rangle$ is the statistical average of operator O, $\mathcal{D}_{suhl}$ is the strength of the four-magnon interaction $c_0 c_0 c_{\mathcal{K}}^\dagger c_{-\mathcal{K}}^\dagger + \text{H.c.}$ [39], and $\Delta\omega_{\pm\mathcal{K}} = \omega_{\pm\mathcal{K}} - \omega_0$. Our model lumps all $\pm\vec{k} \neq 0$ modes into an effective single one [31, 40–43], which we refer to as $\pm\mathcal{K}$ pair. Increasing $\langle n_{\pm\mathcal{K}} \rangle$, e.g. by parametric excitation, should increase τ_0 and reduce f_s.

We considered two thermodynamic baths at possibly different temperatures, T_0 and $T_{\pm\mathcal{K}}$, that interact with the macrospin and $\pm\mathcal{K}$ spin waves, respectively. For a fixed T_0, f_s decreases from the macrospin value when $T_{\pm\mathcal{K}}$ increases [31]. At equilibrium, $T_0 = T_{\pm\mathcal{K}} = T_{env}$, but we may actively control either of the two. An effective increase in $T_{\pm\mathcal{K}}$ can be achieved by parametric excitation of the $\pm\mathcal{K}$ magnons (see Section IV).

The effect of a parametric excitation on $\langle n_{\pm\mathcal{K}} \rangle$ and $\langle n_0 \rangle$ can best be treated in the rotating frame of $\omega_{\pm\mathcal{K}}$ and the

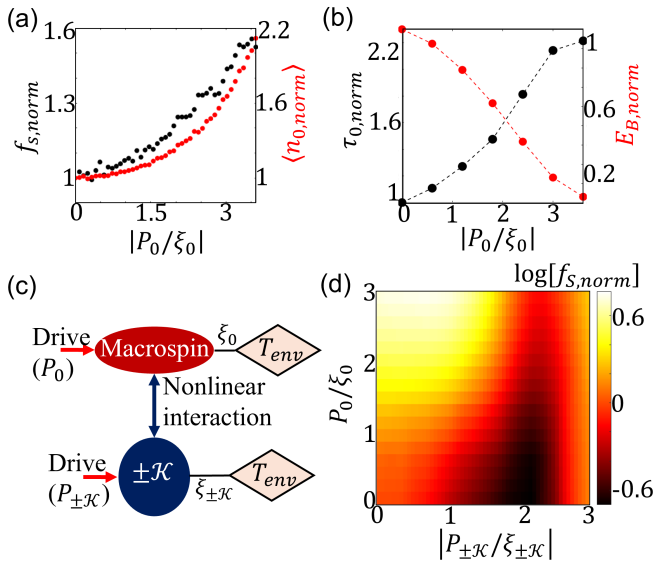

FIG. 1. Parametric excitation and RTN dynamics. (a) $f_{s,norm}$ (black dots) and $\langle n_{0,norm}\rangle$ (red dots) as a function of the microwave drive P_0. (b) $\tau_{0,norm}$ (black dots) and $E_{B,norm}$ (red dots) as a function of P_0. In (a) and (b), only the macrospin is parametrically excited. (c) Schematics of the extended model for parametric excitation of the macrospin and $\pm\mathcal{K}$ magnon pairs and their interaction. (d) $\log f_{s,norm}$ as a function of P_0 and $P_{\pm\mathcal{K}}$ for the model in (c), where 'norm' in the subscripts refers to the normalization by the equilibrium values at $P_0 = P_{\pm\mathcal{K}} = 0$.

model [31],

$$\mathcal{H}_{eff,p} = -\Delta_{\pm\mathcal{K}} c_0^\dagger c_0 + P_{\pm\mathcal{K}}(c_{\mathcal{K}} c_{-\mathcal{K}} + H.c.) + \mathcal{D}^{(Suhl)}(c_0 c_0 c_{\mathcal{K}}^\dagger c_{\mathcal{K}}^\dagger + \text{H.c.}) + \sum_{\vec{k}\in\{0,\pm\mathcal{K}\}} \mathcal{D}_{\vec{k}}^{(Kerr)} c_{\vec{k}}^\dagger c_{\vec{k}} c_{\vec{k}}^\dagger c_{\vec{k}}, \tag{6}$$

where $P_{\pm\mathcal{K}}$ is the amplitude of the parametric drive at $2\omega_{\pm\mathcal{K}}$, and $\mathcal{D}_{\vec{k}}^{(Kerr)}$ is a function of the saturation magnetization M_s, sample thickness, magnetization direction, and wave vector [44].

We chose a perturbative approach, first assuming absence of an interaction between the Kittel mode and the $\pm\mathcal{K}$ pair, viz. $\mathcal{D}^{(Suhl)} = 0$. The equations of motion (EOM) for second order correlation functions lead to the (exact) transcendental equation for $\langle n_{\pm\mathcal{K}}\rangle$

$$4\xi_{\pm\mathcal{K}} {\mathcal{D}_{\pm\mathcal{K}}^{(Kerr)}}^2 \langle n_{\pm\mathcal{K}}\rangle^3 - 4{\mathcal{D}_{\pm\mathcal{K}}^{(Kerr)}}^2 n_{th,\pm\mathcal{K}} \langle n_{\pm\mathcal{K}}\rangle^2 + (\xi_{\pm\mathcal{K}}^2 - 4P_{\pm\mathcal{K}}^2)\langle n_{\pm\mathcal{K}}\rangle - \xi_{\pm\mathcal{K}}^2 n_{th,\pm\mathcal{K}} = 0. \tag{7}$$

The solution when $\langle n_{\pm\mathcal{K}}\rangle \gg n_{th,\pm\mathcal{K}}$ and ${\mathcal{D}_{\pm\mathcal{K}}^{(Kerr)}}^2 \xi_{\pm\mathcal{K}}^4 n_{th,\pm\mathcal{K}}^2 \gg (\xi_{\pm\mathcal{K}}^2 - 4P_{\pm\mathcal{K}}^2)^3$ is

$$\langle n_{\pm\mathcal{K}}\rangle \approx \frac{\xi_{\pm\mathcal{K}}^2 n_{th,\pm\mathcal{K}}}{4{\mathcal{D}_{\pm\mathcal{K}}^{(Kerr)}}^2} + \frac{4P_{\pm\mathcal{K}}^2 - \xi_{\pm\mathcal{K}}^2}{(16{\mathcal{D}_{\pm\mathcal{K}}^{(Kerr)}}^4 \xi_{\pm\mathcal{K}}^2 n_{th,\pm\mathcal{K}})^{1/3}}. \tag{8}$$

The increase of $\langle n_{\pm\mathcal{K}}\rangle$ with $|P_{\pm\mathcal{K}}|$ can be trusted only as long as we may ignore other magnon interactions that kick in at larger excitation powers. The leading order modification is due to a finite Suhl interaction $\mathcal{D}^{(Suhl)}$ that contributes an effective parametric excitation of the Kittel mode in the form of $P_{0,eff} c_0 c_0$+H.c., where

$$P_{0,eff} = \mathcal{D}^{(Suhl)} \langle c_{\mathcal{K}}^\dagger c_{-\mathcal{K}}^\dagger\rangle = \tag{9}$$

$$\mathcal{D}^{(Suhl)} \frac{4iP_{\pm\mathcal{K}}\langle n_{\pm\mathcal{K}}\rangle}{2\xi_{\pm\mathcal{K}} + 4i\mathcal{D}_{\pm\mathcal{K}}^{(Kerr)}\langle n_{\pm\mathcal{K}}\rangle}. \tag{10}$$

A similar third-order polynomial equation as Eq. (7) simplifies to

$$\langle n_0\rangle = \frac{P''}{4\Delta_{\pm\mathcal{K}}|\mathcal{D}_0^{(Kerr)}|} + \frac{\Delta_{\pm\mathcal{K}}^2 n_{th,0}}{P''}. \tag{11}$$

when $\Delta_{\pm\mathcal{K}}\mathcal{D}_0^{(Kerr)} \gg {\mathcal{D}_0^{(Kerr)}}^2\langle n_0\rangle$, $P'' \gg 16\Delta_{\pm\mathcal{K}}^3|\mathcal{D}_0^{(Kerr)}|n_{th,0}$, $\Delta_{\pm\mathcal{K}} > 0$ and $\mathcal{D}_0^{(Kerr)} < 0$. The effectively parametrically driven Kittel mode, in turn, adds a contribution to the parametric drive of the $\pm\mathcal{K}$ pair through the Suhl interaction, modifying it to $P'_{\pm\mathcal{K}} c_{\mathcal{K}} c_{-\mathcal{K}}$ + H.c., where

$$P'_{\pm\mathcal{K}} = P_{\pm\mathcal{K}} + \mathcal{D}^{(Suhl)}\langle c_0^\dagger c_0^\dagger\rangle, \tag{12}$$

$$\langle c_0^\dagger c_0^\dagger\rangle = \frac{-4iP_{0,eff}^*\langle n_0\rangle}{-2\xi_0 + i(2\Delta_{\pm\mathcal{K}} - 4\mathcal{D}_0^{(Kerr)}\langle n_0\rangle)}. \tag{13}$$

For moderate excitations, $(2\Delta_{\pm\mathcal{K}} - 4\mathcal{D}_0^{(Kerr)}\langle n_0\rangle) \gg 2\xi_0$, i.e., $\arg[\langle c_0^\dagger c_0^\dagger\rangle] \approx \arg[P_{0,eff}^*] + \pi$. At relatively large values of $\langle n_{\pm\mathcal{K}}\rangle$, $\arg[P_{0,eff}^*] = \arg[P_{\pm\mathcal{K}}]$, simplifying Eq. (13) to $P'_{\pm\mathcal{K}} \approx P_{\pm\mathcal{K}} - |\mathcal{D}^{(Suhl)}\langle c_0^\dagger c_0^\dagger\rangle|$, which limits $P_{\pm\mathcal{K}}$'s increase by the Suhl interaction.

Summarizing, we expect that $\langle n_{\pm\mathcal{K}}\rangle$ increases with $|P_{\pm\mathcal{K}}|$, but with a diminishing return when $\langle n_0\rangle$ becomes substantial. Therefore, ξ_{corr} should increase continuously with $|P_{\pm\mathcal{K}}|$ and decrease f_s. However, according to Sec. II A, the parametric excitation of the Kittel mode (macrospin) increases f_s. The latter mechanism is first order in $\mathcal{D}^{(Suhl)}$ while the increase in ξ_{corr} is second order in $\mathcal{D}^{(Suhl)}$. Therefore, with increasing excitation power $|P_{\pm\mathcal{K}}|$, f_s should eventually increase again.

We numerically assess the above estimates by computing the dynamics of a model in which the up and down macrospin states interact with $\pm\mathcal{K}$ magnon pairs [31], including the external parametric excitation of both the macrospin and the $\pm\mathcal{K}$ pairs in terms of positive real P_0 and $P_{\pm\mathcal{K}}$, as sketched in Figure 1(c). We adopted $\theta_s = \pi/4$ and $r = 20\,\text{nm}$. $\pm\mathcal{K}$ mode should be the closest to the Kittel mode in frequency, and is taken to be the wave vector with one radial node and parallel to the in-plane equilibrium magnetization. The calculation parameters are then $\omega_{\pm\mathcal{K}} = 4.7\,\text{GHz}$, $\Delta_{\pm\mathcal{K}} = 3.5\,\text{GHz}$, $\mathcal{D}^{(Suhl)} = 8.1\times10^4\,\text{Hz}$, and $\mathcal{D}_{\pm\mathcal{K}}^{(Kerr)} = 1.6\times10^4\,\text{Hz}$. Figure 1(d) is a plot of the resulting $f_{s,norm}$ on a logarithmic

scale. For a fixed $P_{\pm\mathcal{K}}$, f_s increases with increasing P_0 as expected from Sec. II A even in the presence of the interactions. At a fixed P_0 and in line with the theoretical discussion above, f_s depends non-monotonically on $P_{\pm\mathcal{K}}$.

III. MODE-SELECTIVE COOLING

Active cooling of quasiparticles such as phonons by photons [45] can be achieved by feedback [46, 47], Brillouin scattering [48], and radiation pressure interaction [45, 49]. Here the object to be cooled must interact with a degree of freedom that is loosely speaking colder. The radiation pressure $ga^\dagger a(b+b^\dagger)$, where g is the bare interaction strength, can efficiently cool a boson b when $n_{th,a}\approx 0$ and $\xi_a \ll \omega_b$, where ω_a and ω_b are the mode frequencies and ξ_a is the dissipation rate of boson a. Driving the a boson at a frequency that is red shifted from ω_a by ω_b annihilates a b boson by anti-Stokes scattering. The radiation pressure can also cool spin waves [50–54] but cannot be used to cool the $\pm\mathcal{K}$ modes in MTJs. The optical radiation pressure $ga_p^\dagger a_p(c_{\mathcal{K}}+c_{-\mathcal{K}}^\dagger)$, where a_p annihilates a plane-wave photon, does not conserve linear momentum as in case of the cooling by Brillouin scattering described by $b_1^\dagger b_2 c_{\pm\mathcal{K}}$+H.c., where b_1 and b_2 are different and colder bosons than the $\pm\mathcal{K}$ magnons. Feedback cooling also relies on the radiation pressure on $\pm\mathcal{K}$ modes combined with a "beam-splitter" interaction that suffers from the same issue. Here we overcome these limitations by an in-situ cooling mechanism based on a four-magnon interaction that does not constrain the photons.

A. Model

The easy axis anisotropy $\mathcal{H}_{ea}=\gamma H_{K_e} m_z^2$ expanded up to fourth order in the magnon modes $c_{\vec{k}}$, reads

$$\mathcal{H}_{ea}\approx\sum_{\vec{k}}\Big[A_1 c_{\vec{k}}^\dagger c_{\vec{k}}+(A_2 c_{\vec{k}} c_{-\vec{k}}+H.c.)+ c_{\vec{k}}^\dagger c_{\vec{k}}(A_3 c_0+H.c.)+\sum_{\vec{k}'} c_{\vec{k}}^\dagger c_{\vec{k}}(A_4 c_{\vec{k}'} c_{-\vec{k}'}+H.c.)\Big], \tag{14}$$

where $A_{1-4}\propto K_e$ are coefficients. As we discuss in Sec. IV, the voltage-controlled magnetic anisotropy (VCMA) allows a parametric excitation of magnon modes through the second term in Eq. (14) that modulates A_2. VCMA in a nano-MTJ can only excite uniform modes (A_{1-4}) , but it cannot contribute to the momentum matching in terms such as $c_{\vec{k}}^\dagger c_{\vec{k}}(A_3 c_{\pm\mathcal{K}}+H.c.)$ in Eq. (14). A_3 parametrizes the radiation pressure that could help cooling only the Kittel mode. However, we are interested here in cooling the $\pm\mathcal{K}$ modes by A_4 interaction in Eq. (14). To this end we focus on the model

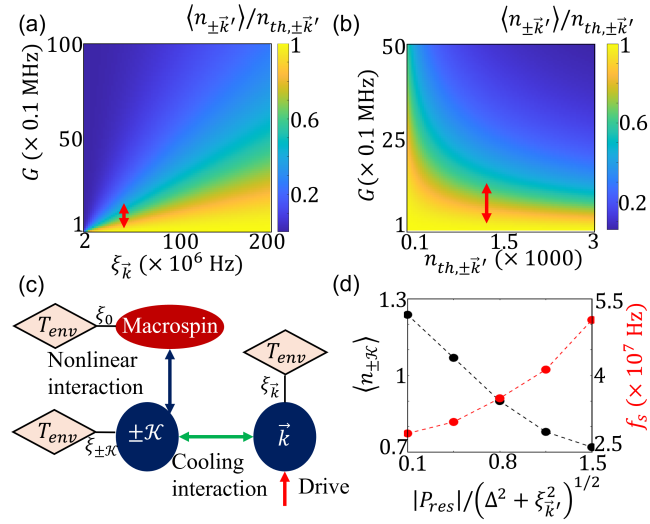

FIG. 2. Magnon cooling and magnetization RTN. (a) Spin wave numbers $\langle n_{\pm\vec{k}'}\rangle/n_{th,\vec{k}'}$ as a function of the dissipation rate $\xi_{\vec{k}}$ of the driven magnon and the interaction strength G. (b) Cooling rate as a function of the initial thermal occupation $n_{th,\pm\vec{k}'}$, and G. (c) The model for magnetization RTN in the presence of the nonlinear interaction and the four-magnon cooling. (d) $\langle n_{\pm\mathcal{K}}\rangle$ (black dots) and f_s (red dots) as a function of the drive amplitude P_{res} ($G\propto P_{res}$). The red double-sided arrows in (a) and (b) indicated the range of G spanned by the drive parameter P_{res} in (d).

$$\mathcal{H}_{cool}=\Delta c_{\vec{k}}^\dagger c_{\vec{k}}+\omega_{\vec{k}'} c_{\vec{k}'}^\dagger c_{\vec{k}'}+ A_4 c_{\vec{k}}^\dagger c_{\vec{k}}(c_{\vec{k}'} c_{-\vec{k}'}+H.c.)+H_{d,\vec{k}}, \tag{15}$$

where $H_{d,\vec{k}}$ drives the $\vec{k}$ mode with frequency ω_d. $\Delta=\omega_{\vec{k}}-\omega_d$ for a resonant and $\Delta=\omega_{\vec{k}}-\omega_d/2$ for a parametric excitation. We adopt a (classical) resonant drive $H_{d,\vec{k}}=P_{res}c_{\vec{k}}+$H.c., where P_{res} is the excitation amplitude. By linearizing $c_{\vec{k}}^\dagger c_{\vec{k}}$ around the mean field of the $\vec{k}$ mode, $c_{\vec{k}}=\alpha_{\vec{k}}+\delta c_{\vec{k}}$, where $\alpha_{\vec{k}}=P_{res}/(\xi_k+i\Delta)$ and $\delta c_{\vec{k}}$ is the fluctuating field operator

$$\mathcal{H}_{cool,eff}=\Delta\delta c_{\vec{k}}^\dagger\delta c_{\vec{k}}+\omega_{\vec{k}'} c_{\vec{k}'}^\dagger c_{\vec{k}'}+ (G\delta c_{\vec{k}}+G^*\delta c_{\vec{k}}^\dagger)(\mathfrak{c}_{\vec{k}'}+H.c.), \tag{16}$$

where $\mathfrak{c}_{\vec{k}'}=c_{\vec{k}'}c_{-\vec{k}'}$, $G=A_4\alpha_{\vec{k}}$. We are free to adopt an $\mathrm{Im}\,\alpha_{\vec{k}}=\mathrm{Im}\,G=0$.

B. Results

The EOMs for $\langle n_{\vec{k}}\rangle$, $\langle n_{\vec{k}'}\rangle$, $\langle\delta c_{\vec{k}}^\dagger\mathfrak{c}_{\vec{k}'}\rangle$, $\langle\mathfrak{c}_{\vec{k}'}^\dagger\mathfrak{c}_{\vec{k}'}\rangle$, and complex conjugates form an approximately closed system of equations. From the Hamiltonian and the Lindblad master equation with linear dissipation, we arrive at the sec-

ond order equation for $\langle n_{\vec{k}'}\rangle$

$$2\xi'_{\vec{k}}D\langle n_{\vec{k}'}\rangle^2 + (-2\xi_{\vec{k}'} - 2\xi_{\vec{k}'}Dn_{th,\vec{k}'} - FG)\langle n_{\vec{k}'}\rangle + 2\xi'_{\vec{k}}n_{th,\vec{k}'} = 0, \quad (17)$$

where

$$D = \frac{BG^2}{\xi_{\vec{k}}} - \frac{2G^4B^2}{\xi_{\vec{k}}C}, \quad (18)$$

$$F = (2BG - \frac{4G^3B^2}{C})n_{th,\vec{k}} + \frac{4\xi_{\vec{k}'}BG}{C}n_{th,\vec{k}'}, \quad (19)$$

$$C = -4\xi_{\vec{k}'} + 2G^2B, \quad (20)$$

$$B = \frac{-(2\xi_{\vec{k}'} + \xi_{\vec{k}})}{(\Delta - 2\omega_{\vec{k}'})^2 + (2\xi_{\vec{k}'} + \xi_{\vec{k}})^2}. \quad (21)$$

Focusing on the anti-Stokes scattering condition $\Delta = 2\omega_{\vec{k}'}$ and assuming the realistic conditions $\{G, \xi_{\vec{k}'}\} \ll \xi_{\vec{k}}$ and $G^4(n_{th,\vec{k}'} - 2n_{th,\vec{k}})^2/\xi^2_{\vec{k}} \ll 4\xi^2_{\vec{k}'}$, Eq. (17) leads to

$$\langle n_{\vec{k}'}\rangle = n_{th,\vec{k}'} - \frac{G^2}{4\xi_{\vec{k}}\xi_{\vec{k}'}}n_{th,\vec{k}'}(n_{th,\vec{k}'} - 2n_{th,\vec{k}}). \quad (22)$$

When G increases, $\langle n_{\vec{k}'}\rangle$ drops below the equilibrium value $n_{th,\vec{k}'}$, cooling the mode $\vec{k}'$. In contrast to radiation pressure, the cooling rate depends on $n_{th,\vec{k}'}$ or T_{env}, being enhanced at higher temperatures for fixed G. Figures 2(a) and (b) illustrate the parameter dependence of the cooling from solving Eq. (17).

To apply the four-magnon scattering as outlined above and cool $\pm\mathcal{K}$ magnons, another mode with thermal occupation $n_{th,\vec{k}} \ll n_{th,\pm\mathcal{K}}$ should be excited to induce $G \neq 0$, and thereby achieve cooling. Therefore, the frequency of the excited mode $\omega_{\vec{k}} \gg \omega_{\pm\mathcal{K}}$, and since both modes are magnons within the same magnet, $\xi_{\vec{k}}/\xi_{\pm\mathcal{K}} \approx \omega_{\vec{k}}/\omega_{\pm\mathcal{K}} \gg 1$ satisfying one of the cooling conditions.

We include another mode ($\vec{k}$) satisfying above conditions to the RTN model [see Fig. 2(c)], and show that τ_s and $\langle n_{\pm\mathcal{K}}\rangle$ decrease with increasing $|P_{res}|$ as predicted. We adopted realistic values of $A_4 = 2\times10^4$, $\omega_{\vec{k}} = 8\omega_{\pm\mathcal{K}}$, $\xi_{\vec{k}} = 8\xi_{\pm\mathcal{K}}$, and $\alpha_G = 0.005$

IV. EXPERIMENTAL CONSIDERATIONS

The macrospin and $\vec{k} \neq 0$ modes may be excited by photons or VCMA [55–59]. Microwave excitation is efficient when the equilibrium magnetization of the MTJ free layer $\vec{m}_{eqb}$ lies in-plane and perpendicular to a stripline under or above the MTJ. Nonlinear phenomena have been observed when exciting magnetic thin films and nano-structures by nano-striplines [60], so it should be possible to achieve the same in MTJs with in-plane magnetizations. For perpendicularly magnetized free layers, microwave parametric excitation would require canting of the magnetization. In Sec. II, we adopted a Zeeman interaction $\mathcal{H}_{ex,ph} = -\gamma\vec{h}_{mw}\cdot\vec{m}$, that for a spatially uniform excitation and easy axis $\|\hat{z}$ simplifies to

$$\mathcal{H}_{ex,ph} = P_{res,ph}c_0 + \sum_{\vec{k}}(P_{p,ph,\vec{k}}c_{\vec{k}}c_{-\vec{k}}) + H.c.,$$
$$P_{res,ph} = \gamma[\frac{h_x}{2}((u_0+v_0)\sin\phi_s - i(u_0-v_0)\cos\theta_s\cos\phi_s) + \frac{h_y}{2}((u_0+v_0)\cos\phi_s - i(u_0-v_0)\cos\theta_s\sin\phi_s) + \frac{h_z}{2}(i(u_0-v_0)\sin\theta_s)],$$
$$P_{p,ph,\vec{k}} = 2\gamma u_{\vec{k}}v_{\vec{k}}[h_x\sin\theta_s\cos\phi_s + h_y\sin\theta_s\sin\phi_s + h_z\cos\theta_s], \quad (23)$$

where θ_s and ϕ_s are polar and azimuthal angles of $\vec{m}_{eqb}$ with respect to the easy axis, $u_{\vec{k}}$ and $v_{\vec{k}}$ parameterize the ellipticity of the magnon modes after a Bogoliubov transformation to magnon annihilation and creation operators $a_{\vec{k}} = u_{\vec{k}}c_{\vec{k}} + v_{\vec{k}}c^\dagger_{-\vec{k}}$ and $a^\dagger_{-\vec{k}} = v^*_{\vec{k}}c_{\vec{k}} + u_{\vec{k}}c^\dagger_{-\vec{k}}$, respectively. In the absence of ellipticity, $v_{\vec{k}} = 0$ and $u_{\vec{k}} = 1$, and parametric excitation is not possible. With increasing $|\vec{k}|$, the exchange interaction dominates, $v_{\vec{k}}$ and consequently $u_{\vec{k}}v_{\vec{k}}$ decrease, and parametric excitation becomes less efficient.

Modulating the magnetic anisotropy by ac electric fields can also efficiently parametrically excite MTJs [58]. When the easy axis is fixed along $\hat{z}$ and the hard axis anisotropy K_h along $\hat{x}$ can be modulated while $\vec{m}_{eqb} \perp \hat{x}$ is at an angle θ_s with respect to the easy axis $\|\hat{z}$,

$$\mathcal{H}_{ex,an,h} = \gamma H_{K_h}(\vec{m}\cdot\hat{x})^2 = \sum_{\vec{k}}(P_{p,an,h,\vec{k}}c_{\vec{k}}c_{-\vec{k}}) + H.c.,$$
$$P_{p,an,h,\vec{k}} = \gamma H_{K_h}u_{\vec{k}}v_{\vec{k}}, \quad (24)$$

On the other hand, modulating the easy axis anisotropy in the same configuration,

$$\mathcal{H}_{ex,an,e} = \gamma H_{K_e}(\vec{m}\cdot\hat{z})^2 = P_{res,an,e}c_0 + \sum_{\vec{k}}(P_{p,an,e,\vec{k}}c_{\vec{k}}c_{-\vec{k}}) + H.c.,$$
$$P_{res,an,e} = 2\gamma H_{K_e}[-i\sqrt{2}\sin\theta_s\cos\theta_s(u_0-v_0)],$$
$$P_{p,an,e,\vec{k}} = \gamma H_{K_e}u_{\vec{k}}v_{\vec{k}}[-4\cos^2\theta_s - \sin^2\theta_s]. \quad (25)$$

In experiments, usually the OOP anisotropy can be modulated. Therefore, for an in-plane magnetized MTJ, $\mathcal{H}_{ex,an,h}$ applies. For perpendicularly magnetized samples, $\mathcal{H}_{ex,an,e}$ applies, and $P_{p,an,e,\vec{k}} \neq 0$ only when the sample has an in-plane crystalline or shape anisotropy.

The cooling mechanism in Sec. III relies on the excitation of a magnon mode $\vec{k}$ at higher frequencies than that of the $\pm\mathcal{K}$ magnons. In nano-MTJs, this requires excitation at few tens of GHz, and twice as high for parametric excitation. Since the ellipticity of the magnons decrease with wave number, the latter would not be as efficient as that of the macrospin (Kittel mode) and the $\pm\mathcal{K}$ magnons, posing an experimental challenge. Smaller

dissipation rates [see Fig. 2(a)] would require a smaller G to achieve the same cooling, and larger anisotropies lead to larger ellipticities and cooling coefficient A_4, which would require smaller drive for the same cooling since $G = |\alpha_{\vec{k}'}|A_4$.

V. CONCLUSION

We propose and formulate active methods to control magnetization RTN in MTJs through magnon fluctuations. We analytically predict and numerically validate RTN attempt times that increase with the parametric excitation power of the macrospin while reducing the energy barrier, effectively accelerating the switching rate. We also show that the parametric excitation of the nonuniform spin waves, despite a non-monotonic power dependence at large excitation amplitudes, generally reduces the RTN frequency. This could be a convenient smoking gun to identify nonlinear interaction effects on RTN. We also propose an in-situ cooling mechanism of nonuniform magnons in MTJs based on driving high-frequency magnon modes that could increase the RTN frequency by an order of magnitude with the current technology. Future work should address complications such as magnetization reversal assisted by domain walls which should become increasingly important for MTJs with larger diameter [6, 8, 35]. We propose concrete experiments that can test the theories, e.g. by parametric excitation of MTJs via ac voltage-controlled modulation of the anisotropy.

ACKNOWLEDGMENTS

We acknowledge support by JSPS KAKENHI (Grants No. 21K13847, No. 19H00645, No. 22H04965, No. 20H02178, No. 23KK0092, No. 24H02231, No. 24H02235, and No. 24H00039), JST-ASPIRE (Grant No. JPMJAP2322), JST PRESTO (Grant No. JPMJPR21B2), MEXT X-NICS (Grant No. JPJ011438), and Cooperative Research Projects of RIEC.

[1] L. Néel, *Theorie du trainage magnetique des ferromagnetiques en grains fins avec application aux terres cuites*, Ann. Geophys. **5**, 99 (1949).

[2] W. F. Brown, *Thermal Fluctuations of a Single-Domain Particle*, Phys. Rev. **130**, 1677 (1963).

[3] W. F. Brown, *Thermal Fluctuations of Fine Ferromagnetic Particles*, IEEE Trans. Mag. **15**, 1196 (1979).

[4] K. Hayakawa, S. Kanai, T. Funatsu, J. Igarashi, B. Jinnai, W. A. Borders, H. Ohno, and S. Fukami, *Nanosecond Random Telegraph Noise in In-Plane Magnetic Tunnel Junctions*, Phys. Rev. Lett. **126**, 117202 (2021).

[5] C. Safranski, J. Kaiser, P. Trouilloud, P. Hashemi, G. Hu, and J. Z. Sun, *Demonstration of Nanosecond Operation in Stochastic Magnetic Tunnel Junctions*, Nano. Lett. **21**, 2040-2045 (2021).

[6] H.-B. Braun, *Thermally Activated Magnetization Reversal in Elongated Ferromagnetic Particles*, Phys. Rev. Lett. **71** , 3557 (1993).

[7] H.-B. Braun, *Statistical mechanics of nonuniform magnetization reversal*, Phys. Rev. B **50**, 16501 (1994).

[8] S. Krause, G. Herzog, T. Stapelfeldt, L. Berbil-Bautista, M. Bode, E.Y. Vedmedenko, and R. Wiesendanger, *Magnetization Reversal of Nanoscale Islands: How Size and Shape Affect the Arrhenius Prefactor*, Phys. Rev. Lett. **103**, 127202 (2009).

[9] S. Kanai, K. Hayakawa, H. Ohno, and S. Fukami, *Theory of relaxation time of stochastic nanomagnets*, Phys. Rev. B **103**, 094423 (2021).

[10] K. Y. Camsari, R. Faria, B. M. Sutton, and S. Datta, *Stochastic p-Bits for Invertible Logic*, Phys. Rev. X **7**, 031014 (2017).

[11] W. A. Borders, A. Z. Pervaiz, S. Fukami, K. Y. Camsari, H. Ohno, and S. Datta, *Integer factorization using stochastic magnetic tunnel junctions*, Nature **573**, 390-393 (2019).

[12] D. Vodenicarevic, N. Locatelli, A. Mizrahi, J. S. Friedman, A. F. Vincent, M. Romera, A. Fukushima, K. Yakushiji, H. Kubota, S. Yuasa, S. Tiwari, J. Grollier, and D. Querlioz, *Low-Energy Truly Random Number Generation with Superparamagnetic Tunnel Junctions for Unconventional Computing*, Phys. Rev. Appl. **8**, 54045 (2017).

[13] A. Mizrahi, T. Hirtzlin, A. Fukushima, H. Kubota, S. Yuasa, J. Grollier, and D. Querlioz, *Neural-like computing with populations of superparamagnetic basis functions*, Nat. Commun. **9**, 1533 (2018).

[14] J. Kaiser, W. A. Borders, K. Y. Camsari, S. Fukami, H. Ohno, and S. Datta, *Hardware-Aware In Situ Learning Based on Stochastic Magnetic Tunnel junctions*, Phys. Rev. Appl. **17**, 014016 (2022).

[15] N. S. Singh, K. Kobayashi, Q. Cao, K. Selcuk, T. Hu, S. Niazi, N. A. Aadit, S. Kanai, H. Ohno, S. Fukami, K. Y. Camsari, *CMOS plus stochastic nanomagnets enabling heterogeneous computers for probabilistic inference and learning*, Nat. Commun. **15**, 2685 (2024).

[16] J. Si, S. Yang, Y. Cen, J. Chen, Y. Huang, Z. Yao, D.-J. Kim, K. Cai, J. Yoo, X. Fong, H. Yang, *Energy-efficient superparamagnetic Ising machine and its application to traveling salesman problems*, Nat. Commun. **15**, 3457 (2024).

[17] K. Watanabe, B. Jinnai, S. Fukami, H. Sato, and H. Ohno, *Shape anisotropy revisited in single-digit nanometer magnetic tunnel junctions*, Nat. Commun. **9**, 663 (2018).

[18] B. Jinnai, K. Watanabe, S. Fukami, and H. Ohno, *Scaling magnetic tunnel junction down to single-digit nanometers-Challenges and prospects*, Appl. Phys. Lett. **116**, 160501 (2020).

[19] J. Igarashi, B. Jinnai, K. Watanabe, T. Shinoda, T. Funatsu, H. Sato, S. Fukami, and H. Ohno, *Single-nanometer CoFeB/MgO magnetic tunnel junctions with*

high-retention and high-speed capabilities, npj Spintronics **2**, 1 (2024).

[20] T. Hioki, H. Shimizu, T. Makiuchi, and E. Saitoh, *State tomography for magnetization dynamics*, Phys. Rev. B **104**, L100419 (2021).

[21] T. Makiuchi, T. Hioki, Y. Shimazu, Y. Oikawa, N. Yokoi, S. Daimon, and E. Saitoh, *Parametron on magnetic dot: Stable and stochastic operation*, Appl. Phys. Lett. **118**, 022402 (2021)

[22] M. Elyasi, E. Saitoh, and G. E. W. Bauer, *Stochasticity of the magnon parametron*, Phys. Rev. B **105**, 054403 (2022).

[23] D. Lachance-Quirion, S. P. Wolski, Y. Tabuchi, S. Kono, K. Usami, and Y. Nakamura, *Entanglement-based single-shot detection of a single magnon with a superconducting qubit*, Science **367**, 425 (2020).

[24] M. Elyasi, Y. M. Blanter, G. E. W. Bauer, *Resources of nonlinear cavity magnonics for quantum information*, Phys. Rev. B **101**, 054402 (2020).

[25] H. Yuan, Y. Cao, A. Kamra, R. A. Duine, and P. Yan, *Quantum magnonics: When magnon spintronics meets quantum information science,* Phys. Rep. **965**, 1 (2022).

[26] B. Z. Rameshti, S. V. Kusminskiy, J. A. Haigh, K. Usami, D. Lachance-Quirion, Y. Nakamura, C.-M. Hu, H. X. Tang, G. E. W. Bauer, and Y. M. Blanter, *Cavity magnonics*, Phys. Rep. **979**, 1 (2022)

[27] A. Chumak et al., *Advances in magnetics roadmap on spin-wave computing*, IEEE Trans. Magn. **58**, 1 (2022).

[28] H. A. Kramers, *Brownian motion in a field of force and the diffusion model of chemical reactions*, Physica **7**, 284 (1940).

[29] S. Kanai, K. Hayakawa, M. Elyasi, K. Kobayashi, J. Igarashi, B. Jinnai, W. A. Borders, G. E. W. Bauer, H. Ohno, and S. Fukami1, *Stochastic switching time constant and instability in nanomagnets*, submitted.

[30] H. Kaneko, R. Ota, K. Kobayashi, S. Kanai, M. Elyasi, G. E. W. Bauer, H. Ohno, and S. Fukami, *Temperature dependence of the properties of stochastic magnetic tunnel junction with perpendicular magnetization*, APEX **17**, 053001 (2024).

[31] M. Elyasi, S. Kanai, H. Ohno, S. Fukami, and G. E. W. Bauer, *Effect of nonlinear magnon interactions on stochastic magnetization switching*, Phys. Rev. B **110**, 094433 (2024).

[32] S. Arrhenius, *Über die Reaktionsgeschwindigkeit bei der Inversion von Rohrzucker durch Säuren*, Zeitschrift für Physikalische Chemie. **4U**, 226 (1889).

[33] D. E. Endean, C. T. Weigelt, R. H. Victora, and E. Dan Dahlberg, *Tunable random telegraph noise in individual square permalloy dots*, Appl. Phys. Lett. **104**, 252408 (2014).

[34] P. Talatchian, M. W. Daniels, A. Madhavan, M. R. Pufall, E. Jue, W. H. Rippard, J. J. McClelland, and M. D. Stiles, *Mutual control of stochastic switching for two electrically coupled superparamagnetic tunnel junctions*, Phys. Rev. B **104**, 054427 (2021).

[35] L. Soumah, L. Desplat, N.-T. Phan, A. S. E. Valli, A. Madhavan, F. Disdier, S. Auffret, R. Sousa, U. Ebels, and P. Talatchian, *Nanosecond stochastic operation in perpendicular superparamagnetic tunnel junctions*, arXiv:2402.03452v1.

[36] P. Kinsler and P. D. Drummond, *Quantum dynamics of the parametric oscillator*, Phys. Rev. A **43**, 6194 (1991).

[37] H. J. Carmichael, *Statistical Methods in Quantum Optics 2*, Springer (2008).

[38] D. F. Walls and G. J. Milburn, *Quantum Optics*, Springer (2008).

[39] H. Suhl, *The Theory of Ferromagnetic Resonance at High Signal Powers*, Phys. Chem. Solids **1**, 209 (1957).

[40] V. S. Lvov, *Wave Turbulence Under Parametric Excitation*, (Springer-Verlag, 1994).

[41] S. M. Rezende, *Fundamentals of magnonics*, Springer, Berlin, (2020).

[42] O. Lee, K. Yamamoto, M. Umeda, C. W. Zollitsch, M. Elyasi, T. Kikkawa, E. Saitoh, G. E. W. Bauer, H. Kurebayashi, *Nonlinear magnon polaritons*, Phys. Rev. Lett. **130**, 046703 (2023).

[43] T. Makiuchi, T. Hioki, H. Shimizu, K. Hoshi, M. Elyasi, K. Yamamoto, N. Yokoi, A. Serga, B. Hillebrands, G. E. W. Bauer, and E. Saitoh, *Persistent magnetic coherence in magnets*, Nat. Mater. (2024).

[44] P. Krivosik and C. E. Patton, *Hamiltonian formulation of nonlinear spin-wave dynamics: Theory and applications*, Phys. Rev. B **82**, 184428 (2010).

[45] M. Aspelmeyer, T. J. Kippenberg, and F. Marquardt, *Cavity optomechanics*, Rev. Mod. Phys. **86**, 1391 (2014).

[46] S. Mancini, D. Vitali, and P. Tombesi, *Optomechanical Cooling of a Macroscopic Oscillator by Homodyne Feedback*, Phys. Rev. Lett. **80**, 688 (1998).

[47] M. Koch, C. Sames, A. Kubanek, M. Apel, M. Balbach, A. Ourjoumtsev, P. W. H. Pinkse, and G. Rempe, *Feedback Cooling of a Single Neutral Atom*, Phys. Rev. Lett. **105**, 063806 (2011).

[48] M. Tomes, F. Marquardt, G. Bahl, and T. Carmon, *Quantum-mechanical theory of optomechanical Brillouin cooling*, Phys. Rev. A **84**, 063806 (2011).

[49] P.-F. Cohadon, A. Heidmann, and M. Pinard, *Cooling of a mirror by radiation pressure*, Phys. Rev. Lett. **83**, 3174 (1999).

[50] A. Osada, R. Hisatomi, A. Noguchi, Y. Tabuchi, R. Yamazaki, K. Usami, M. Sadgrove, R. Yalla, M. Nomura, and Y. Nakamura, Cavity Optomagnonics with Spin-Orbit Coupled Photons, Phys. Rev. Lett. 116, 223601 (2016)

[51] X. Zhang, N. Zhu, C.-L. Zou, and H. X. Tang, Optomagnonic Whispering Gallery Microresonators, Phys. Rev. Lett. 117, 123605 (2016).

[52] J. A. Haigh, A. Nunnenkamp, A. J. Ramsay, and A. J. Ferguson, Triple-Resonant Brillouin Light Scattering in Magneto-Optical Cavities, Phys. Rev. Lett. 117, 133602 (2016).

[53] S. Viola Kusminskiy, H. X. Tang, and F. Marquardt, *Coupled spin-light dynamics in cavity optomagnonics*, Phys. Rev. **A** 94, 033821 (2016).

[54] S. Sharma, Y. M. Blanter, and G. E. W. Bauer, Light scattering by magnons in whispering gallery mode cavities, Phys. Rev. B96, 094412 (2017).

[55] J. Zhu et al., *Voltage-induced ferromagnetic resonance in magnetic tunnel junctions*, Phys. Rev. Lett. **108**, 197203 (2012).

[56] B. Rana, Y. Fukuma, K. Miura, H. Takahashi, and Y. Otani, *Excitation of coherent propagating spin waves in ultrathin CoFeB film by voltagecontrolled magnetic anisotropy*, Appl. Phys. Lett. **111**, 52404 (2017).

[57] R. Verba, V. Tiberkevich, I. Krivorotov, and A. Slavin, *Parametric excitation of spin waves by voltage-controlled magnetic anisotropy*, Phys. Rev. Appl. **1**, 044006 (2014).

[58] Y.-J. Chen et al., *Parametric resonance of magnetization excited by electric field*, Nano Lett. **17** 572 (2017).

[59] B. Rana, S. Choudhury, K. Miura, H. Takahashi, A. Barman, and Y. Otani, *Electric field control of spin waves in ultrathin CoFeB films*, Phys. Rev. B **100**, 224412 (2019).

[60] L. Sheng, M. Elyasi, J. Chen, W. He, Y. Wang, H. Wang, H. Feng, Y. Zhang, I. Medlej, S. Liu, W. Jiang, X. Han, D. Yu, J.-P. Ansermet, G. E. W. Bauer, H. Yu, *Nonlocal Detection of Interlayer Three-Magnon Coupling*, Phys. Rev. Lett. **130**, 046701 (2023).